Corrosion Science 88 (2014) 481–486

Contents lists available at ScienceDirect

Corrosion Science

journal homepage: www.elsevier.com/locate/corsci

Short Communication

High-throughput corrosion quantification in varied microenvironments

Matthew J. Whitfield [a], David Bono [a,b,c], Lei Wei [c], Krystyn J. Van Vliet [a,b,*]

[a] Department of Materials Science and Engineering, Massachusetts Institute of Technology, Cambridge, MA 02139, USA
[b] Department of Biological Engineering, Massachusetts Institute of Technology, Cambridge, MA 02139, USA
[c] Research Laboratory of Electronics, Massachusetts Institute of Technology, Cambridge, MA 02139, USA

ARTICLE INFO

Article history:
Received 15 April 2014
Accepted 22 July 2014
Available online 2 August 2014

Keywords:
A. Carbon steel
C. Oxidation
C. Microbiological corrosion
C. Passive films

ABSTRACT

Harsh conditions ranging from those of biomedical implants to industrial oilfield applications prompt rapid assessment of whether and to what extent corrosion will occur. Here, we describe and demonstrate a novel high-throughput approach to quantify corrosion susceptibility based upon electrical resistance and colorimetric outputs. We illustrate this capability by quantifying aerobic corrosion rates of steel alloys within hours, and by comparing anaerobic microbiologically influenced corrosion (MIC) conditions over several days. Such methods can be extended to rapidly assess conditions that will accelerate corrosion, to compare corrosion mitigation scenarios, and to explore biofilm formation and MIC mechanisms through robust replicate conditions.

1. Introduction

As technological advancement enables us to access increasingly harsh environments, ranging from implanted biomedical devices to undersea oil and gas deposits, we continue to test the limits of corrosion susceptibility and require quantitative insights to predict and extend structural reliability. The highly complex nature of corrosion processes, as well as the wide range of relevant environmental variables, complicates rigorous identification of corrosion susceptibility. For example, despite mitigation attempts, microbiologically-influenced corrosion (MIC) and associated biofilm formation (biofouling) have been implicated in several rapidly progressing, high-profile failures of buried steel pipeline [1–4]. While sulfate reducing bacteria (SRB) are considered a main culprit in anaerobic environments, the complex consortium of microbial species and the biofilms they produce have obviated mechanistic conclusions. Despite much research of the microbiology and the engineering effects, the mechanisms by which MIC enhances ferrous corrosion and the appropriate strategies to mitigate MIC corrosive loss remain elusive [5,6].

The limitations of prevailing experimental techniques to quantify and predict corrosion in controlled environments have led to the development of several higher-throughput measurement methods (see two recent review articles [7,8]). Current high-throughput approaches use either a single metal bulk substrate with areas controllably exposed to different microenvironments [9,10], deposited metallic thin films in each microenvironment [11–13], or multiple electrode systems (2 or 3) within each microenvironment [14–18]. While existing high-throughput methods hold tremendous promise in certain conditions, their production is not necessarily straightforward and scalable, and their applicability for biotic studies which require complete isolation between microenvironments to prevent cross-contamination and a continuous surface for bacterial colonization is unclear.

Here we describe a high-throughput corrosion testing platform that assays corrosion susceptibility of metals by tracking the changing resistance of thin wires and colorimetric changes of the surrounding solution within a 96-well format. While resistance-based probes have been validated as an effective means to measure corrosion at much larger scales with only a few samples [19–21], multiplexing of these measurements enables more rapid consideration of corrosion susceptibility and rates that requires only sub-mL-scale volumes of fluid. This approach allows for independent control of cues – including chemical composition of surrounding medium, gas concentrations, temperature, type and number of microbial species. Results are obtainable over the course of hours to days. We validate this approach through consideration of low-carbon steel corrosion in both aerobic and anaerobic environments, and in both abiotic and biotic conditions.

2. Experimental

2.1. Multiplexed platform

We designed a novel multiplexed platform to measure in parallel the electrical resistance of metallic samples placed within a

* Corresponding author at: Laboratory for Material Chemomechanics, 8-237, 77 Massachusetts Ave., Cambridge, MA 02139. Tel.: +1 617 253 3315.
E-mail address: krystyn@mit.edu (K.J. Van Vliet).

http://dx.doi.org/10.1016/j.corsci.2014.07.045
0010-938X/

range of controlled fluid microenvironments (see Supplemental methods for a detailed platform description). The multiplexer had 384 addressable channels, used here to conduct 96, 4-wire resistance measurements when coupled with an Agilent 34420A micro-ohm meter. A set a ribbon cables connected the multiplexer to a "test fixture" circuit board designed to sit directly on top of a 96-well plate suspending a u-shaped wire loop within each well. To align the 96-well plate and the test fixture, an aluminum frame was constructed; this allowed the wire array to lower into the center of each well and then hold the two together tightly. The frame also allowed light to pass through wells, as required for optical imaging. Labview 2013 was used to control data acquisition. An Arduino 1.5.4 macro was used to set the current channel on the multiplexer. After setting the channel, the ohmmeter was triggered to begin taking measurements. The voltmeter was set to the 1 Ω range with an integration time of 20 power line cycles and offset compensation. At each time point, five measurements were taken for each channel and averaged after discarding the highest and lowest measurement. All 96 wells could be assessed in this manner in 8 min 15 s (5.15 s/channel).

2.2. Metal sample preparation

Two sources of low carbon steel (1008, McMaster Carr) were used for experiments: a 27 gauge (361 μm diameter) wire used in the as-received condition, and a 12 gauge (2.05 mm diameter) wire drawn into thinner wire segments (see Supplemental methods). The thin black oxide coating on the wires was removed by light sanding with 1500 grit sandpaper and then cleaned by wiping with 70% ethanol. The wire was cut to approximate size and shaped into a "u"-shape by winding tightly between a series of posts of 3.68 mm diameter. This step provided uniform curvature and microstructural damage (due to plastic deformation upon bending) to all wires. Wire diameter was assessed via optical microscopy at a magnification of 20×. Before corrosion susceptibility experiments, the wires were again cleaned and sterilized by soaking in 70% ethanol for 10 min.

2.3. Corrosion assays and analysis

The 96-well plate format allowed us to independently control both the fluid microenvironments and the chemical composition or microstructure of the metal wire within each well. Thus 96 separate experiments were conducted in parallel (a set of experiments, with the potential for replicates of a given condition within that set). Sets were performed either aerobically on the bench top or anaerobically within an anaerobic incubator. Prior to the start of each experiment, baseline resistance values were recorded for each channel before liquid was added. In order to start experiments in all wells at the same initial time point, a 96-well plate was prepared before immersing the wires, with each well containing 300 μL liquid volume of the desired composition. Eight wells per set were maintained as "dry" (devoid of fluid) no-corrosion controls for baseline reading fluctuations. For anaerobic experiments, both the bacterial medium and purified water (18.2 MΩ cm) were deoxygenated by boiling for 5 min under a stream of nitrogen. Stock solutions of the various salt concentrations (w/v) were prepared by dissolving NaCl in purified water at the appropriate ratio.

Timelapsed imaging in aerobic conditions was performed with a Nikon D90 camera taking images every 10 min, controlled through a computer using the data acquisition software DCamCapture. A light source and diffusing filter were placed above the 96-well plate and the camera below to capture the light transmitted through each well. The average greyscale pixel intensity of each well was calculated over time and normalized by the pixel intensity of control wells (no liquid) using ImageJ. In anaerobic conditions, a Canon Powershot A490 digital camera enabled running intervalometer scripts without the need of an attached computer. Images were acquired every 10 min and analyzed in ImageJ.

For post-corrosion assay imaging, optical light microscopy was conducted on an inverted microscope in fluid (Olympus IX-81) and an upright microscope in ambient air (Olympus BX53) and scanning electron microscopy was conducted in low vacuum (JEOL 6610LV).

2.4. Microbe culture

Desulfovibrio vulgaris, a strain of sulfate reducing bacteria (SRB), were purchased from ATCC (29579) and grown in ATCC #1249 Modified Barr's Medium containing 0.06% cysteine in an anaerobic chamber (Shel Lab BacBASIC) at 30 °C in a 5% hydrogen, 5% carbon dioxide, 90% nitrogen atmosphere. The medium was prepared without Component IV, such that the wire was the only iron source. The original freeze-dried stock was added to medium, allowed to grow for six days until high turbidity and strong H_2S smell were observed, and then frozen down in 10% DMSO to create the frozen SRB stock used for subsequent experiments. Prior to corrosion experiments, 10 mL of medium was inoculated with bacteria from frozen stock and allowed to expand for six days in an anaerobic incubator.

3. Results and discussion

3.1. Rationale for high-throughput resistance and colorimetric platform

Corrosion of metals involves the loss of structural metal atoms from the bulk to the ionic or complexed forms. A system that can detect very small amounts of material loss could therefore rapidly assess corrosion. Here we employ two techniques to achieve this sensitivity to corrosion susceptibility: the resistance change of thin u-shaped wires loops and the color change of the surrounding fluid medium. Because the resistance of a wire is based on the material resistivity (constant at a given temperature), the length of the wire (constant), and the cross-sectional area (changes with corrosion), monitoring a change in resistance can assess the degree to which the cross-sectional area has decreased due to corrosion (Fig. 1A). Additionally, the darkness and hue of the surrounding medium can give an indication of the course of corrosion and corrosive product. Taken together, they can provide a rapid assessment of the rate, course, and type of corrosion occurring. Fig. 1B shows an example of the change of resistance and a visual representation of a wire corroding in an aerobic salt solution. Correspondingly, the wire exhibited a visible decrease in diameter as the corrosion proceeded.

The 4-wire resistance measurements in Fig. 1B were taken with an Agilent 34420A micro-ohm meter, which nominally has noise of 1–2 μΩ. However, even when using low-resistance Kelvin probes, taking measurements on more than a single wire per experiment required manually attaching, detaching, and replacing the leads; this repeated manual manipulation caused resistance measurements to vary by milliohms among repeated measurements, rendering sensitivity insufficient. Additionally, the time required to move the leads between different experimental wires limited the time resolution of measurements and obfuscated long-term resistance tracking. Therefore, we next designed a high-throughput integrated platform.

3.2. Design of a high-throughput corrosion detection system

An automated system was designed and constructed, consisting of a multiplexer to controllably address a series of channels and a

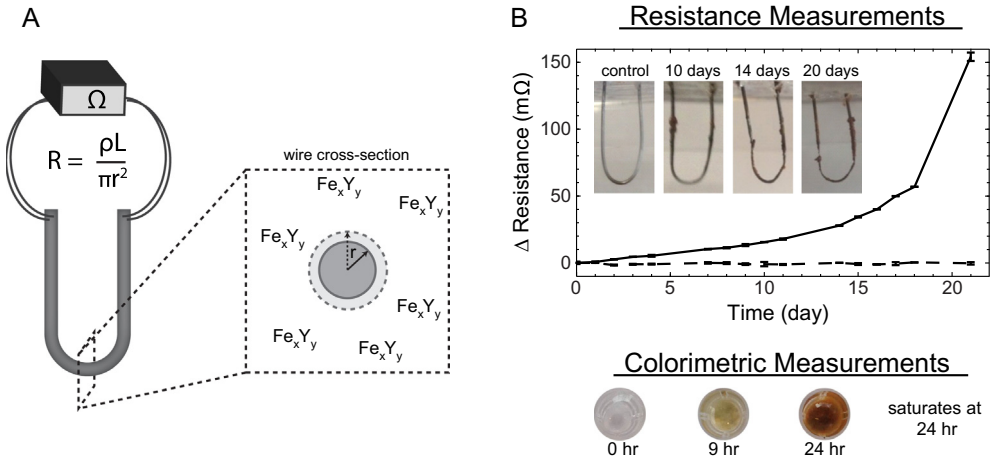

Fig. 1. Wire resistance and medium color changes provide an indicator of corrosion. (A) The resistance R of a thin wire is determined by its resistivity ρ, length L, and cross-sectional area (defined by the radius as πr^2) and can be determined by a 4-wire measurement. As the cross-sectional area decreases during corrosion, the resistance increases as corrosion removes metal from the wire which complexes with other atoms on the metal surface or in solution. Those corrosion products may be of the form Fe_xA_y where A may be, for example, sulfur or oxygen; x and y indicate stoichiometry. (B) As an example, a u-shaped wire loop placed in a salt solution (phosphate buffered saline) visibly thins over time, accompanied by an increase in the resistance of the wire (solid line). The resistance of a control wire that was maintained in air does not change (dashed line). Error bars are standard error of the mean. The color and brightness of the surrounding medium also changes as iron atoms leave the metal forming, in this case, iron oxides exhibiting the typical orange-red color of rust.

"test fixture" with integrated 4-wire leads to hold a series of experimental wires (Fig. 2; see Methods). When connected to the micro-ohm meter and computer, this essentially clones the meter for each channel without requiring any manual intervention. This approach allowed us to individually acquire resistance measurements in serial for wires within each well of a 96-well plate at each time point. An upward facing time lapse camera allowed the simultaneous recording of any color changes of the medium.

3.3. Abiotic, aerobic corrosion in salt conditions

As an initial validation of the system, the resistance change of a 361 μm diameter steel wire in the presence of a range of sodium chloride concentrations was measured in aerobic conditions. Each column of the 96-well array represented replicates of a different condition: air, distilled water, and salt concentrations from 1% to 7% (w/v). Thus there were eight replicates per condition. By monitoring the wires for a period of time in air, the baseline resistance (28–34 mΩ) and signal to noise ratio (~1800:1) were determined (see Supplementary results and Fig. S1A–C). Thus, in theory, this approach using this wire diameter could detect corrosion rates of 1, 0.1, and 0.01 mm/year within 30 min, 5 h, and 2 days, respectively.

At time zero, the appropriate liquids were added to the wells. Fig. 3A shows the average and standard error of the mean for each condition, demonstrating that corrosion could be detected within 1 h and distinctions made among different salt concentrations. Fig. 3B shows the resistance change and corrosion rate at a time point 3 h after the addition of the aqueous solutions. The corrosion rate was estimated by calculating the change in wire radius with time, assuming uniform corrosion occurring equally around the circumference of the wire along its full length. Thus, based upon the wire parameters (resistivity ρ and length L) and the change from an initial resistance R_o to a resistance R_t at a later time t, the corrosion rate is given as:

$$\text{Corrosion Rate}\left(\frac{mm}{yr}\right) = \frac{\Delta\text{radius}}{\Delta t} = \frac{\sqrt{\frac{\rho L}{\pi}}\left[\frac{1}{\sqrt{R_o}} - \frac{1}{\sqrt{R_t}}\right]}{\Delta t}.$$

Both the salt concentration dependence and the estimated corrosion rate were in agreement with previous studies that required more time and more sample volume [22,23], thus supporting the rapid estimation of corrosion susceptibility and rate in this multiplexed high-throughput format. The process of acquiring the resistance measurements via continuous data acquisition did not noticeably affect the corrosion, as control wires exhibited indistin-

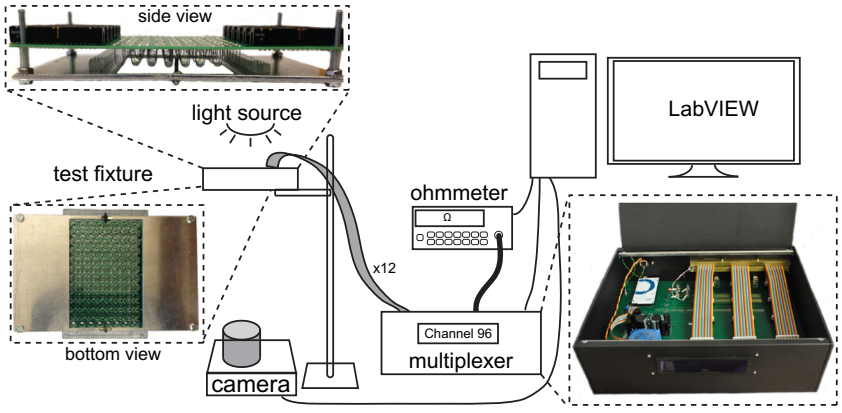

Fig. 2. Schematic of constructed high-throughput corrosion detection system.

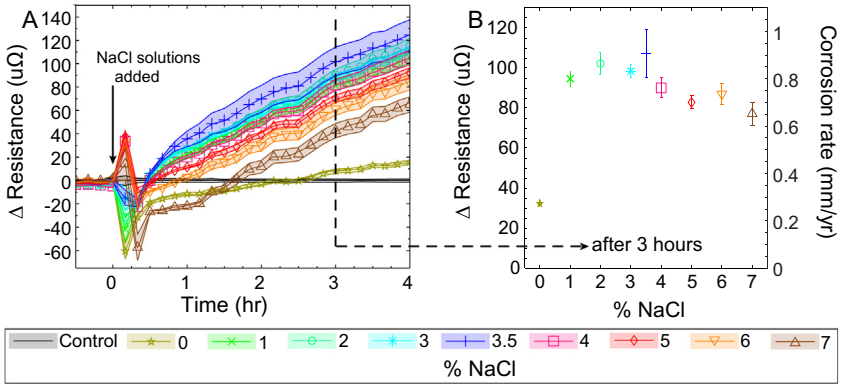

Fig. 3. Wire resistance changes during abiotic, aerobic corrosion in aqueous saline solutions. (A) Average resistance change of wires in purified water containing NaCl in concentrations from 0% to 7% (*w*/*v*) as indicated by legend. Eight wires per condition. (B) The resistance change (left axis) and estimated corrosion rate (right axis) after 3 h for each NaCl concentration (same legend).

guishable resistance changes when placed within the same microenvironments but with measurements taken at only a few discrete time points over the same total experiment duration (Fig. S2).

Concurrent with these resistance measurements, colorimetric data were also collected. These images were quantified by changes in greyscale intensity (with negative values indicating darker images) (Fig. 4). In the context of this aerobic saline environment, this colorimetric indicator was less sensitive than resistance, in that the well brightness decreased within the first 30 min but no distinction was possible among varying salt concentrations. The colorimetric signal also saturated within one day as the corrosion products settled to the bottom of the wells. However, the mechanistic complementarity of these colorimetric data for even a well-studied model corrosion environment can be appreciated, in that the orange hue of the precipitate is indicative of Fe_xO_y corrosion products.

Another set of experiments was conducted with iron wires drawn to various diameters (from 65 to 361 μm), all in 3.5% NaCl saline solutions. With decreasing wire diameter, the resistance increased faster and the signal noise became higher (Fig. S3A–C), although the corrosion rate was approximately the same for all but the smallest wires over the first few hours (again, estimated from the change in wire radius) (Fig. S3D). Those spurious corrosion rates for the smallest drawn wires are attributable to imperfections induced in the wire drawing and wire extraction process, which naturally contributed more strongly to measured resistance of smallest-diameter wires. While the manufacturing process could still be improved to produce wires of sub-100 μm diameter, these data demonstrate the ability to multiplex corrosion susceptibility and corrosion rate measurements on a metal not readily available in the desired wire form. This sample preparation method could be considered for other ductile metals and alloys. However, it should be noted that microstructural changes induced by the drawing process may also modulate corrosion susceptibility; in such cases, this wire processing could limit direct application of these results to industrially prevalent material microstructures.

3.4. Anaerobic corrosion in the presence of sulfate reducing bacteria

We next assayed corrosion in biotic environments, specifically anaerobic aqueous environments comprising sulfate reducing bacteria (SRBs). Biofilms produced by such SRBs readily form on the low carbon steel wires. As Fig. 5 demonstrates, wires can be non-destructively imaged while still in fluid, producing an *in situ* pseudo cross-sectional view from which the morphology and thickness of the biofilm/corrosion product can be quantified. Drying the wire and then rinsing with ethanol to remove loosely bound precipitates allows further assessment of the biofilm and/or underlying metal surface if sections of the biofilm are mechanically removed. Further, scanning electron microscopy *ex situ* allows individual bacteria within the biofilm to be discerned. Because the multiplexed design allows for many replicate trials within a single experiment, individual wires can be sacrificed at various time points to characterize biofilm formation and corrosion progression without interrupting the overall experimental set.

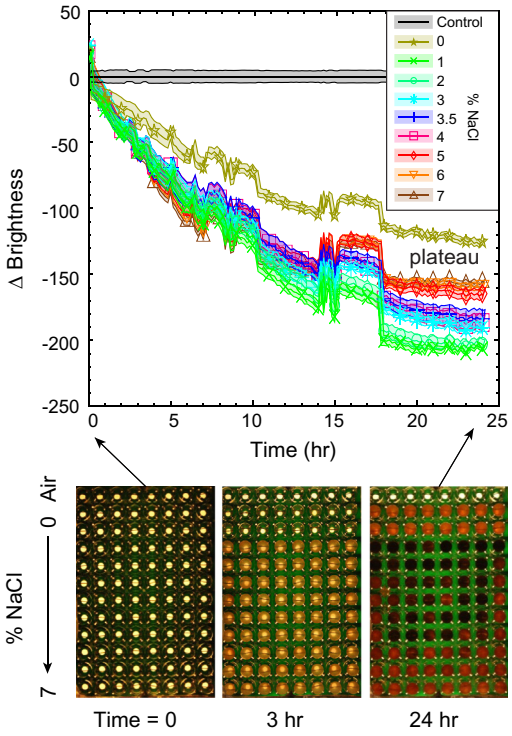

Fig. 4. Corresponding colorimetric changes during abiotic, aerobic corrosion in aqueous saline solutions. The average darkening of the medium in NaCl concentrations from 0% to 7% (*w*/*v*) as indicated by legend. The salt solutions can be distinguished from the purified water but not from each other. The color signature saturates within one day. Shaded area and error bars ± standard error of the mean. View of the entire plate at time 0, after 3 h, and after 24 h.

Fig. 6 demonstrates a systematic consideration of nutrient availability on the SRB corrosion susceptibility of these materials. Using the thinner drawn steel wires (115 μm mean diameter), nutrient conditions ranged from completely depleted (bacteria

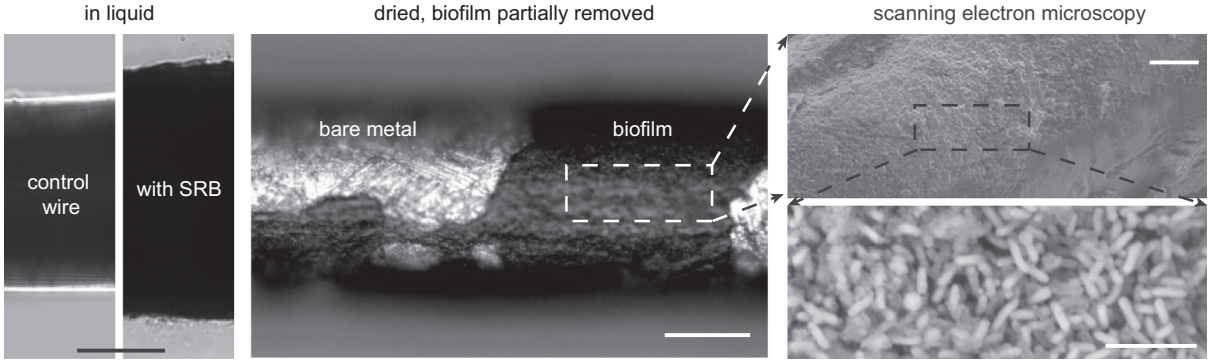

Fig. 5. Biofilm formation on wires in anaerobic conditions. Imaging biofilm-coated wires while in liquid provides a pseudo cross-sectional view allowing the biofilm corrosion/product to be readily observed in comparison to a control wire in same conditions without SRBs (initial wire diameters 117 μm). Light and scanning electron microscopy of the dried wire allows further assessment of biofilm and underlying metal morphology. Scale bars 50 μm for optical microscopies and 10 μm (1500×) and 5 μm (5500×) for the upper and lower electron microscopy images, respectively.

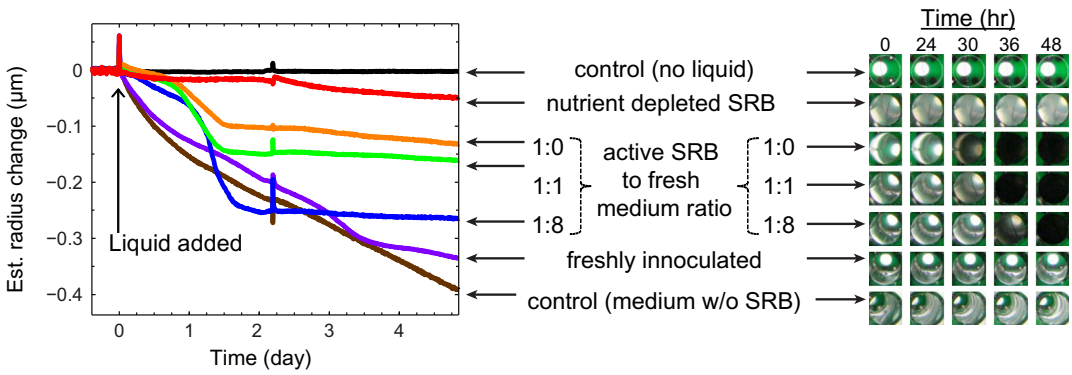

Fig. 6. Corrosion in anaerobic aqueous environments comprising sulfate reducing bacteria (SRBs). The estimated radius change for wires in indicated conditions of differing nutrient availability (see Fig. S4 for measurement error) along with colorimetric data at the indicated time points for the same conditions. Data shown as estimated radius change, and not resistance change, to normalize for small differences in initial wire diameter among wells.

grown for a month with no medium exchange) to newly inoculated in fresh media. Intermediate to these extremes of bacterial metabolic activity, varying volumes of fresh media were added to bacteria that had just reached their stationary phase after 6 days of growth (as assessed by turbidity). The higher the nutrient availability, the greater the corrosion extent by day 4 (indicated as an estimated radius change). Furthermore, after an initial corrosion rate peak between days 1 and 2 of up to 0.19 mm/year, the corrosion reached a plateau for SRB conditions at various points after the day 1, consistent with nutrient depletion. The corresponding colorimetric data in Fig. 6 complemented these results: black corrosion product indicated iron sulfides rather than iron oxides. The well color rapidly transitioned to black and saturated between days 1 and 2 for conditions with a metabolically active population of SRBs. Freshly inoculated wells turned dark by day 4, and other conditions did not indicate a change in color (and thus a colorimetrically undetectable extent of corrosion over the duration assayed).

Interestingly, all SRB conditions appeared to be passivating at most time points, as compared to the SRB-free medium control. This is likely the case because, despite our attempts to create a truly anaerobic environment, minute concentrations of oxygen below our detection limit (1000 ppm) can facilitate slow oxidative corrosion. In the absence of fluid flow, the biofilms thus appeared to limit the oxygen exposure to the metal surface. The corrosion rate of the control environment was only 0.03 mm/year, or 20- to 30-fold slower than that observed in aerobic aqueous saline conditions. The maximum average measured corrosion rate of the MIC environments was 0.028 mm/year, occurring for conditions that promoted high SRB metabolic activity. In other words, for these specific SRB and environments, MIC included biofilm formation and was slower than abiotic corrosion for low-oxygen environments, and was significantly slower than aerobic corrosion of the same metals in saline environments.

While it is possible that the conductivity of the biofilm itself could mask corrosion-induced resistance increases, our additional control experiments indicated this unlikely to be a compounding factor. SRB biofilms grown on glass capillaries in ferrous ion-containing medium demonstrated that while the biofilm could be conductive, the electrical resistance was still orders of magnitude higher than that of the steel wires used in our experiments (data not shown). Furthermore, growth of ferrous ion-containing biofilms on platinum wires (a metal with extremely low corrosion susceptibility) did not detectibly increase measured conductivity (data not shown).

3.5. Advantages and limitations

The use of wire in corrosion assays provides several advantages over existing approaches that make it amenable to rapid, high-throughput corrosion analysis. First, wire forms can be adapted easily to almost any conformation, allowing use in confined environments such a 96 well plates and microfluidic channels. Second, the small sample volumes allow rapid assessment of corrosion when compared to traditional studies conducted on larger (cm- to m-scale) samples over the course of months, without the need to scale up metal manufacturing or sourcing of the fluid (such as that from produced water of potential and current oil wells). In addition, wires can be imaged easily, even providing an *in situ*

pseudo cross-sectional view of the corrosion process. In other words, this approach allows rapid, systematic identification of the least/most susceptible metal composition or microstructure or of the least/most corrosive fluid composition. Such capabilities are well-suited to corrosion susceptibility screening.

The current platform also has certain constraints. Each well contains a static environment with no continuous fluid exchange. While liquid can be exchanged manually through a small hole above each well without interrupting the experiment, corrosion in environments with continuous fluid flow cannot be studied. This also leads to saturation of the colorimetric signal as corrosion products build up and settle to the well floor. Because each well is not sealed completely, evaporation can occur over several days and gas exchange is possible between wells. Future designs incorporating pumps could allow for controlled fluid and gas flow, as well as controlled removal of gaseous byproducts of corrosion or biotic metabolism. Because test materials must be fabricated in wire format, some materials may be precluded from use with this system. Further, resistance measurements alone cannot easily distinguish between uniform and pitting corrosion, although samples can be sacrificed at desired time points to visually assess corrosion modes. Finally, it is important to note that the estimated corrosion rate is sensitive to pitting, as the resistance is modulated by the areas of smallest cross-section.

4. Conclusions

A novel high-throughput approach for the rapid assessment of corrosion susceptibility has been achieved for up to 96 wire samples analyzed in parallel, through the use of resistance and colorimetric changes. The capabilities of this multiplexed approach were demonstrated by assessing the effect of NaCl concentration on aerobic, abiotic corrosion and of nutrient availability on anaerobic, biotic corrosion for a low carbon steel. This platform could be used as a screening mechanism with conditions of interest studied further via other techniques.

These multiplexed electrical/colorimetric analyses are also well suited to studies that leverage directed mutagenesis of bacteria. Such studies could provide insights into the mechanisms by which microbes enhance corrosion or by which antimicrobial reagents work most effectively, but require 100s-1000 s of independent experiments. Thus, to consider corrosive environments of increasing complexity, the rapid and quantitative measurements afforded by this multi-well format can expedite discovery of corrosion susceptibility and also of corrosion mitigation options.

Acknowledgements

This work was funded by the MIT Energy Initiative (MITEI)-BP Energy Research Fund and the MRSEC Program of the National Science Foundation under award number DMR-0819762. Finally, we gratefully acknowledge helpful discussions with K. Wunch and A. Cockerill (BP), J. Wall and G. Zane (U. Missouri) for advice on culture of SRBs, and the expertise of Y. Fink (MIT) whose customized preform-to-fiber draw tower was used to manufacture the steel wires of smallest diameter described in this work.

Appendix A. Supplementary material

Supplementary data associated with this article can be found, in the online version, at http://dx.doi.org/10.1016/j.corsci.2014.07.045.

References

[1] G. Abraham, V. Kain, G.K. Dey, MIC failure of type 316 L seawater pipeline, Mater. Performance 48 (2009) 64–69.
[2] F.P. Yu, J.J. Dillon, T.P. Henry, Identification and control of microbiologically influenced corrosion in a power plant, Corrosion 2010, 14–18 March, NACE International, San Antonio, TX.
[3] M. Egan, Internal corrosion suspected as cause of alaskan pipeline leak, Mater. Performance 50 (2011) 14–23.
[4] S. Al-Jaroudi, A. Ul-Hamid, M. Al-Gahtani, Failure of crude oil pipeline due to microbiologically induced corrosion, Corros. Eng., Sci. Technol. 46 (2011) 568–579.
[5] Z. Augustinovic, O. Birketveit, Microbes–oilfield enemies or allies?, Oilfield Rev 24 (2012) 4–17.
[6] D. Enning, J. Garrelfs, Corrosion of iron by sulfate-reducing bacteria: new views of an old problem, Appl. Environ. Microbiol. 80 (2014) 1226–1236.
[7] S. Taylor, The investigation of corrosion phenomena with high throughput methods: a review, Corros. Rev. 29 (2011) 135–151.
[8] T. Muster, A. Trinchi, T. Markley, D. Lau, P. Martin, A. Bradbury, A. Bendavid, S. Dligatch, A review of high throughput and combinatorial electrochemistry, Electrochim. Acta 56 (2011) 9679–9699.
[9] P. White, A. Hughes, S. Furman, N. Sherman, P. Corrigan, M. Glenn, D. Lau, S. Hardin, T. Harvey, J. Mardel, High-throughput channel arrays for inhibitor testing: proof of concept for AA2024-T3, Corros. Sci. 51 (2009) 2279–2290.
[10] P. White, G. Smith, T. Harvey, P. Corrigan, M. Glenn, D. Lau, S. Hardin, J. Mardel, T. Markley, T. Muster, A new high-throughput method for corrosion testing, Corros. Sci. 58 (2012) 327–331.
[11] M. Fleischauer, T. Hatchard, G. Rockwell, J. Topple, S. Trussler, S. Jericho, M. Jericho, J. Dahn, Design and testing of a 64-channel combinatorial electrochemical cell, J. Electrochem. Soc. 150 (2003) A1465–A1469.
[12] J. He, J. Bahr, B.J. Chisholm, J. Li, Z. Chen, S.V.N. Balbyshev, V. Bonitz, G.P. Bierwagen, Combinatorial materials research applied to the development of new surface coatings X: a high-throughput electrochemical impedance spectroscopy method for screening organic coatings for corrosion inhibition, J. Comb. Chem. 10 (2008) 704–713.
[13] T. Markley, S. Dligatch, A. Trinchi, T. Muster, A. Bendavid, P. Martin, D. Lau, A. Bradbury, S. Furman, I. Cole, Multilayered coatings: tuneable protection for metals, Corros. Sci. 52 (2010) 3847–3850.
[14] B. Chambers, S. Taylor, M. Kendig, Rapid discovery of corrosion inhibitors and synergistic combinations using high-throughput screening methods, Corrosion 61 (2005) 480–489.
[15] B. Chambers, S. Taylor, High-throughput assessment of inhibitor synergies on aluminum alloy 2024–T3 through measurement of surface copper enrichment, Corrosion 63 (2007) 268–276.
[16] N.D. Budiansky, F. Bocher, H. Cong, M. Hurley, J.R. Scully, Use of coupled multi-electrode arrays to advance the understanding of selected corrosion phenomena, Corrosion 63 (2007) 537–554.
[17] T. Muster, A. Hughes, S. Furman, T. Harvey, N. Sherman, S. Hardin, P. Corrigan, D. Lau, F. Scholes, P. White, A rapid screening multi-electrode method for the evaluation of corrosion inhibitors, Electrochim. Acta 54 (2009) 3402–3411.
[18] S. Kallip, A. Bastos, M. Zheludkevich, M. Ferreira, A multi-electrode cell for high-throughput SVET screening of corrosion inhibitors, Corros. Sci. 52 (2010) 3146–3149.
[19] R. Royer, R. Unz, Use of electrical resistance probes for studying microbiologically influenced corrosion, Corrosion 58 (2002).
[20] R. Royer, R. Unz, Influence of ferrous iron on the rate and nature of microbiologically influenced corrosion of high-strength steel under sulfate-reducing conditions, Corrosion 61 (2005) 1070–1077.
[21] S. Li, Y.-G. Kim, S. Jung, H.-S. Song, S.-M. Lee, Application of steel thin film electrical resistance sensor for in situ corrosion monitoring, Sensor Actuators B: Chem. 120 (2007) 368–377.
[22] H. Uhlig, M. Morrill, Corrosion of 18–8 stainless steel in sodium chloride solutions, Ind. Eng. Chem. 33 (1941) 875–880.
[23] H. Möller, E. Boshoff, H. Froneman, The corrosion behaviour of a low carbon steel in natural and synthetic seawaters, J. S. Afr. Inst. Min. Metall. 106 (2006) 585–592.